Catalysis Today 142 (2009) 165–169

Contents lists available at ScienceDirect

Catalysis Today

journal homepage: www.elsevier.com/locate/cattod

# Photocatalytic decomposition of acetone over dc-magnetron sputtering supported vanadia/$TiO_2$ catalysts

Ş Neaţu [a], E. Sacaliuc-Pârvulescu [a,b], F. Lévy [b], V.I. Pârvulescu [a,*]

[a] University of Bucharest, Department of Chemical Technology and Catalysis, B-dul Regina Elisabeta 4-12, Bucharest 030016, Romania
[b] Ecole Polytechnique de Lausanne, Department of Physics, 1015 Lausanne, Switzerland

ARTICLE INFO

*Article history:*
Available online 1 October 2008

*Keywords:*
Titania photocatalyst
Acetone photodecomposition
dc-Sputtering deposition of vanadium
XRD
Raman
AFM

ABSTRACT

Two series of titania-based photocatalysts were prepared by the sputtering method, in pure Ar atmosphere at a pressure of 0.5 Pa using a vanadium target source in a direct dc mode with a discharge of 300 V. The time of deposition was varied between 1 and 10 min in order to obtain different thickness of vanadium films. The first catalysts series (samples V/$TiO_2$(A)-*n*) was prepared deposing vanadium on pure $TiO_2$ anatase, while for the second series (samples V/$TiO_2$(AR)-*n*) the deposition was made onto $TiO_2$ Degussa P25. The samples have been investigated by means of vibrational (DRIFT and Raman) and optical (UV–vis in the DRS mode). Chemical analysis of the samples was made using the ICP-AES technique, while the crystalline structure of the deposed films onto the $TiO_2$ supports was checked by X-ray diffraction (XRD). The samples morphology was analyzed using the AFM microscopy. The photocatalytic decomposition of acetone was considered as a reaction test. The activity of the investigated catalysts was found to be influenced by both the amount of vanadium and the support nature. Among the investigated catalysts V/$TiO_2$(AR)-32 nm exhibited the higher activity. The activity of this catalyst was also superior to that of $TiO_2$ Degussa P25.



## 1. Introduction

For the last decade, environmental issues have been pressed governments and scientific communities to allocate more attention to research and development. As a result of these efforts, the use of heterogeneous semiconductor materials for photocatalytic decontamination emerged as a very attractive solution. Usually, to be effective in practice, these materials should exhibit high activity for wide environmental applications such as both air clean-up and water purification [1]. Among the various oxide semiconductor photocatalysts, titanium dioxide has been proven to be the most suitable for environmental applications due to its beneficial characteristics: high photocatalytic efficiency, the appropriate energy bands configuration for charge transfer at the interface and absorption in near UV range, biological and chemical inertness, strong oxidizing power, low cost and toxicity, and long-term stability against photo- and chemical corrosion. In addition to its wide band gap, titanium dioxide exhibits many other interesting properties, such as transparency to visible light, a high refractive index and a low absorption coefficient [2–4]. All these characteristics make it very useful in a wide range of applications [5–7], including photo-decomposition of noxious compounds found in the atmosphere and in water [5,8–11]. To decrease the charge recombination and increase the $TiO_2$ photocatalytic efficiency, inorganic ions [12,13], noble metals [14], or other semiconductor metal oxides [15] have been loaded on the surface or into the crystal lattice of photocatalysts. Such modification can change semiconductor surface properties by altering interfacial electron-transfer events and thus the photocatalytic efficiency. Intimately mixed aerogels of $TiO_2$–$SiO_2$ with the incorporation of transition metal ions V, Cr, Mn, Fe, and Ni were investigated for the decomposition of acetaldehyde under UV irradiation [16]. The reaction rates for V and Mn were nearly 5 and 10 times, respectively than their corresponding rate constants under visible light irradiation. However, these authors found that the activity of these catalysts under UV light irradiation is double that of the standard Degussa P25 $TiO_2$ catalyst. These results indicate that the extent of dispersion and local structure of the metal oxides play a significant role in the decomposition reaction of acetaldehyde under visible as well under UV light irradiation.

The aim of this study was to investigate the preparation of vanadium $TiO_2$-doped photocatalysts using the dc-magnetron

* Corresponding author. Tel.: +40 21 4100241; fax: +40 21 4100241.
*E-mail address:* v_parvulescu@yahoo.com (V.I. Pârvulescu).

0920-5861/$ – see front matter © 2008 Elsevier B.V. All rights reserved.
doi:10.1016/j.cattod.2008.08.034

sputtering technique and to check the effect of the preparative conditions on the catalysts properties and photocatalytic behaviour in decomposition of acetone. Commercial titanium dioxides were used as support. The sputtering technique is a versatile deposition method, allowing the preparation of thin films with controlled crystallinity, composition (including ion doping) and thickness. In this process, atoms from a target (cathode) connected to a voltage source are sputtered off by positively charged ions originating in the plasma created between the cathode and the anode (substrate holder).

## 2. Experimental

### 2.1. Catalyst preparation

Vanadium thin films have been deposited onto two commercial $TiO_2$ ceramic supports (pure titania anatase from Sachtleben Chemie GmbH and $TiO_2$ Degussa P25) by dc-magnetron sputtering. The deposition was made in pure Ar atmosphere at a pressure of 0.5 Pa using a V (99.99%) target from Metals Research Ltd. (diameter 35 mm) in direct dc mode with a discharge of 300 V. The distance between the substrate holder and the vanadium target inside the deposition chamber was 11 cm. The substrates temperature was kept at room temperature during deposition.

The substrate supports were polished before the deposition of V films. The time of deposition was varied between 1 and 10 min in order to obtain different thickness of vanadium films onto $TiO_2$ supports. To ensure a uniform deposit, the substrate was rotated with a high speed (3000 rot./min). Thin films of V were also deposited on silicon substrates for thickness calibration. The resulting samples were denoted as V/$TiO_2$(A)-*n* and V/$TiO_2$(AR)-*n*, where *n* indicates the thickness of the vanadium film while A and R denote the anatase and rutile allotropic forms of $TiO_2$.

### 2.2. Catalyst characterization

Chemical analysis of the samples was determined using the ICP-AES technique, the crystalline structure and of the V films on $TiO_2$ supports was investigated by X-ray diffraction (XRD) in both Bragg-Brentano and grazing incidence geometries ($\Omega = 5^\circ$), with a Rigaku diffractometer using the monochromatized Cu Kα radiation ($\lambda = 1.5418$ Å). The thickness of the deposited films was determined using an Alphastep 500 surface profile from Tencor Instruments. The surface morphology was checked in air by atomic force microscopy (AFM, Topometrix Explorer). The samples have been investigated by means of vibrational (DRIFT and Raman) and optical (UV–vis in the DRS mode) spectroscopies. DRIFT spectra were collected, at a 4 $cm^{-1}$ spectral resolution, in reflectance mode with a Nicolet 4700 spectrometer from Thermo Electron. Raman spectra were collected with a LabRAM HR UV–Visible–NIR (200–1600 nm) Raman Microscope Spectrometer from Horiba Jobin Yvon equipped with a DL785-100 laser emitting at 785 nm. The laser power adopted during the measurements was set just to guarantee the best compromise between the best S/N ratio and the stability (verified by means of several test measurements) of the samples under the laser beam. In the present case 10% of the total laser power was employed. The photons scattered by the sample were dispersed by a 1200 lines/mm grating monochromator and simultaneously collected on a CCD camera. The collection optic was set at 20× objective. Each spectrum corresponds to the sum of 50 acquisitions each of them during 10 s. Diffuse reflectance spectra (DRS) in the range of 200–1100 nm were taken on a Specord 250 spectrophotometer from Analytic Jena. The spectra were recorded against a spectralon hallow as the baseline under ambient conditions. The band gap energy ($E_g$) for allowed transitions was determined by finding the intercept of the straight line in the low-energy rise of a plot of $[F(R) \cdot h\nu]^2$ against $h\nu$, where $F(R)$ is the Kubelka–Munk reemission function, and $h\nu$ is the incident photon energy [17]. XPS spectra were recorded at room temperature using a SSX-100 spectrometer, Model 206 from Surface Science Instrument. The pressure in the analysis chamber during the analysis was 1.33 mPa. Monochromatized Al Kα radiation ($h\nu = 1486.6$ eV) was used. It was generated by bombarding the Al anode with an electron gun operated with a beam current of 12 mA and acceleration voltage of 10 kV. The spectrometer energy scale was calibrated using the Au $4f_{7/2}$ peak centered at 83.98 eV. Charge correction was made with the C 1s signal of adventitious carbon (C–C or C–H bonds) located at 284.8 eV.

### 2.3. Photocatalytic tests

Photocatalytic tests were performed in a flow system, using a water-cooled quartz reactor. The catalysts were irradiated using a Philips HPK 125W UV-lamp. The incident light flux was 0.156 mmol quanta/s, as measured by uranyl-oxalic actinometry [18]. The quartz walls of the photoreactor determined lower limit of entering light (about 365 nm cut-off filter). The photoreactor was cooled by a stream of air, which allowed maintaining the reaction temperature at 26–28 °C. Catalytic tests used dc-magnetron sputtering films deposited on $TiO_2$(A) and $TiO_2$(AR) platelets and $TiO_2$ Degussa P25 as reference. Catalyst platelets were placed in the reactor, perpendicular to the light propagation direction. Air purified, dried and saturated with acetone (99.6%, Aldrich) was blown into the reactor with a flow rate of 5 $cm^3$ $min^{-1}$. The gas flow was maintained constant during the experiments using a pump. The reactor was coupled to a Fisher–Rosemount on line gas analyzer, equipped with a $CO_2$ detector. The gas analyzer was calibrated before each test. Before UV irradiation, acetone-containing air was purged through the reactor over the catalysts for 20 min. No catalytic reaction products were detected in the absence of the UV irradiation. The start of UV irradiation was taken as the initial moment of each catalytic experiment. The reaction products were analyzed using a Trace GC 2000 equipped with a DSQ MS system from Thermo Electron. Photocatalytic experiments used the same surface area of the platelets, i.e. 2.25 $cm^2$. The activity of the investigated photocatalysts was calculated as the number of mmoles of acetone transformed in $CO_2$ per $cm^2$ of photocatalyst. In order to check the reproducibility of photocatalytic behaviour, each sample was tested in several runs. The exposure time was at least 100 min in order to check the catalysts stability.

## 3. Results and discussion

Table 1 compiles the film layer thickness of the investigated photocatalysts for the different deposition times. As expected the increase of the deposition time was accompanied by an increase of the film thickness.

Fig. 1 shows the XRD patterns for the V/$TiO_2$ photocatalysts prepared using $TiO_2$(A). All samples exhibited the well-developed

**Table 1**
Film layer thickness of the investigated photocatalysts for the different deposition times

| | Time of V deposition (min) | | | | | |
|---|---|---|---|---|---|---|
| | 0 | 1 | 2 | 4 | 7 | 10 |
| Film thickness V/$TiO_2$(A) | 0 | 1.84 | 3.7 | 14 | 25 | 33 |
| Film thickness V/$TiO_2$(AR) | 0 | 1.85 | 4 | 15 | 22 | 32 |

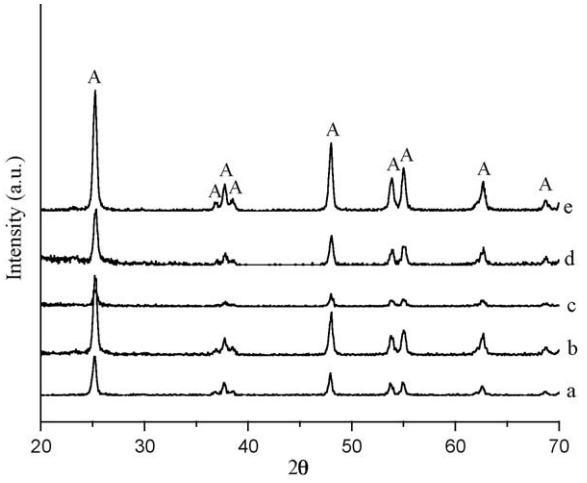


**Fig. 1.** X-ray diffraction patterns of V/$TiO_2$(A)-*n* catalysts: (a) $TiO_2$(A)-support, (b) V/$TiO_2$(A)-3.7 nm, (c) V/$TiO_2$(A)-14 nm, (d) V/$TiO_2$(A)-25 nm and (e) V/$TiO_2$(A)-33 nm.

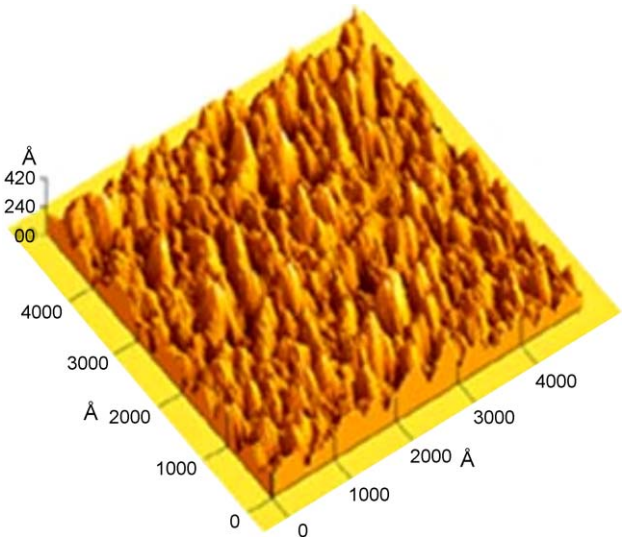


**Fig. 3.** AFM picture of V/$TiO_2$(AR)-32 nm photocatalyst.

lines of the anatase structure. For the samples prepared using $TiO_2$(AR) the X-ray diffraction patterns (Fig. 2) revealed the coexistence of two phases, i.e. anatase (A) and rutile (B) in the $TiO_2$ support. The comparison of the XRD patterns of the parent samples with those of the prepared V–$TiO_2$ samples shown that the dc-magnetron sputtering deposition of vanadium did not cause relevant damages in crystallinity. The XRD patterns of V/$TiO_2$ catalysts with different vanadium film thicknesses did not showed lines corresponding to V-containing crystalline phases irrespective of the quantity of V on the support. This may account for a high dispersion of vanadium in these films.

Fig. 3 shows the AFM picture of the V/$TiO_2$(AR)-32 nm photocatalyst. The morphology showed in this figure is actually the morphology of the $TiO_2$(AR) support. In addition to data obtained by XRD, AFM analysis showed that, indeed, vanadium deposition occurred without the modification of the morphology of the parent support. The deposition resulted as a thin film, covering uniformly the surface of the support without any agglomeration. The same behaviour was observed for the V–$TiO_2$(A) samples too.

Figs. 4 and 5 show DRS spectra of the V/$TiO_2$(A) and V/$TiO_2$(AR) reference materials, respectively. In the UV–Vis region, the $TiO_2$(A) and $TiO_2$ (AR) supports possesses absorption thresholds at ~400 and ~410 nm, respectively, which is due to the ligand–metal charge-transfer (LMCT) transitions between $Ti^{4+}$ and oxygen ligands, such as –OH, –O–Ti. These absorption thresholds correspond to band gaps of 3.10 and 3.02 eV, respectively. The presence of vanadium changed the spectrum of titania in the visible region. The V/$TiO_2$ samples exhibit absorptions thresholds between 420 and 460 nm that correspond to band gaps in the range 2.95–2.69 eV. These absorptions apparently originate from the overlapped LMCT transitions of both V and Ti cations (electronic transitions from oxygen 2p orbitals to vanadium/titanium 3d orbitals). Taking in account that no d–d transitions are observed in the DRS spectra we could assume that oxidation state of vanadium is 5+. This supposition was confirmed by the XPS measurements that showed a symmetric peak located at 517.6 eV that can be assigned to V(V) species. The increase in the V content reduces the reflectance and produces a red shift of the absorption edge of titania. This behavior is ascribed to the fact that vanadium can narrow the band gap of titania by ~0.4 eV, making the catalyst capable to use UV–vis radiation of lower energy.

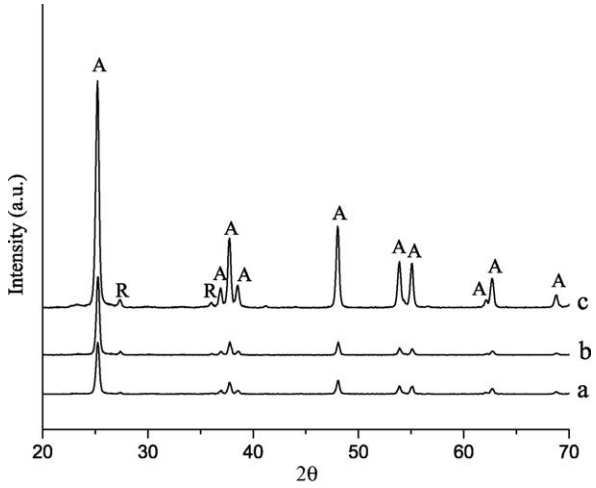


**Fig. 2.** X-ray diffraction patterns of V/$TiO_2$(AR)-*n* catalysts: (a) $TiO_2$(AR)-support, (b) V/$TiO_2$(AR)-15 nm and (c) V/$TiO_2$(AR)-22 nm.

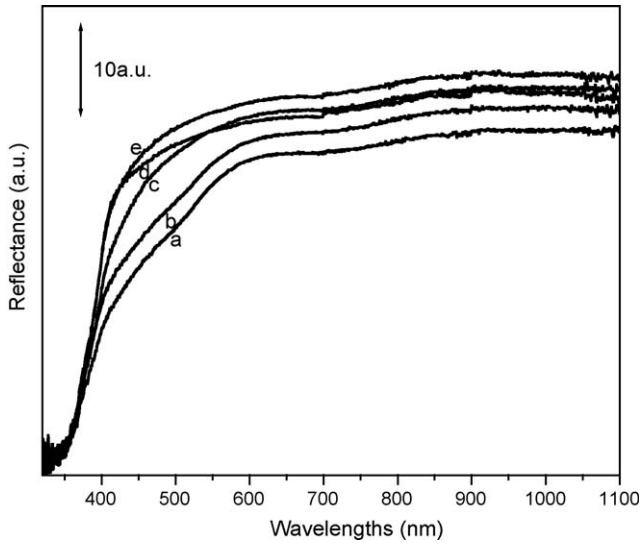


**Fig. 4.** UV–vis DRS spectra of the reference materials: (a) V/$TiO_2$(A)-33 nm, (b) V/$TiO_2$(A)-25 nm, (c) V/$TiO_2$(A)-14 nm, (d) V/$TiO_2$(A)-3.7 nm, and (e) $TiO_2$(A)-support.

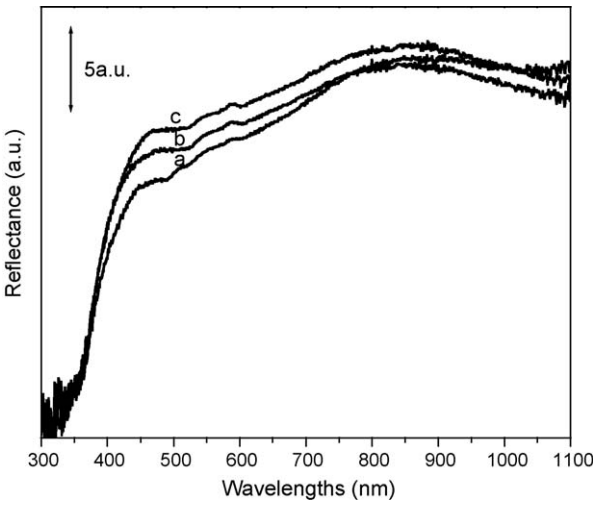


**Fig. 5.** UV–vis DRS spectra of the reference materials: (a) V/$TiO_2$(AR)-22 nm, (b) V/$TiO_2$(AR)-15 nm, and (c) $TiO_2$(AR)-support.

Fig. 6 shows the Raman spectrum recorded under ambient conditions for V/$TiO_2$(AR)-32 nm. The spectrum of vanadia containing sample shows the presence of the vanadium in different coordinations: i.e. as terminal $O_3$(V=O) and polymeric V–O–V species. Thus, peaks at 950, and 1030 $cm^{-1}$ can be assigned to V–O–V, and terminal V=O stretching vibrations of the isolated $VO_4$ species [25–27]. The relative ratios of these bands slightly changed with the vanadium loading. No band assigned to microcrystalline $V_2O_5$ has been detected.

Table 2 compiles the photocatalytic data. As can be seen from the presented results, the both pure $TiO_2$ supports (anatase and anatase/rutile mixture) showed similar photocatalytic activities for photodegradation of acetone. It can be also observed that the activity of the V/$TiO_2$ samples begins to increase with the increase of vanadium loading. A deposition time smaller than 7 min led to a slight decrease in the activity of those photocatalysts if there are compared with the pure $TiO_2$ supports. Increasing the deposition time corresponds to a positive effect. The maximum in activity was reached for the photocatalysts prepared by deposition times of 10 min.

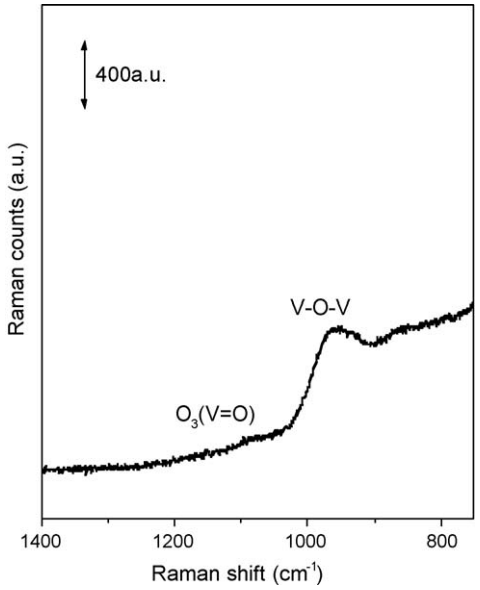


**Fig. 6.** Raman spectrum of V/$TiO_2$(AR)-32 nm sample.

**Table 2**
Activity of the investigated photocatalysts after 100 min UV irradiation (mmoles mineralized acetone/$cm^2$ photocatalyst) in photodecomposition of acetone

| | Time of V deposition (min) | | | | | |
|---|---|---|---|---|---|---|
| | 0 | 1 | 2 | 4 | 7 | 10 |
| V/$TiO_2$(A) | 0.20 | 0.18 | 0.13 | 0.16 | 0.36 | 0.98 |
| V/$TiO_2$(AR) | 0.20 | 0.07 | 0.07 | 0.22 | 0.60 | 1.00 |

Comparing the two types of supports used in this study, the decomposition rate is generally lower for the pure anatase support catalysts. Such behaviour was assigned to the fact that when anatase interweaves rutile, the anatase electrons will be transferred to rutile, while the holes will be transferred from rutile to anatase [28]. In this way the anatase/rutile mixed phase will hinder the electron–hole recombination. On the other side, because of its narrower band gap, the rutile phase is extending the useful range of the photoresponse and will harvest more light [29].

Correlating the band gap with the photocatalytic activity it resulted that the higher photocatalytic activity was achieved by the samples with the lowest $E_g$ values (Fig. 7). It results that the catalytic performance is proportional to the catalyst capacity to use UV–vis radiation of lower energy. The UV light activity of the V/$TiO_2$ may be caused due to band gap narrowing by mixing the V 3d and Ti 3d states with O 2p states, respectively. Increasing the band gap over 2.9 eV had no influence on the photocatalytic activity. The activity of the photocatalysts showing higher band gaps was almost similar.

The photocatalytic oxidation of acetone started after first attaining adsorption equilibrium. The DRIFT spectra of V/$TiO_2$ taken at different reaction times are displayed in Fig. 8. The spectrum of V/$TiO_2$ before photodecomposition of acetone was used as a reference and subtracted from those recorded during photocatalytic oxidation. These results show that under UV irradiation the intensity of the acetone bands (negative peaks at 1689 and 1054 $cm^{-1}$) progressively decreases, and simultaneously new strong peaks arise at 2976, 2931, 1714, 1557, 1445, and 1420 $cm^{-1}$. Some of these positive bands can be related to formate ($HCOO^-$) and bidentate acetate ($CH_3$–$COO^-$) surface complexes [19–21]. The peak at 1716 $cm^{-1}$ can be assigned to the $\nu$(C=O) vibration mode of adsorbed aldehyde. Both formaldehyde and acetaldehyde are plausible intermediates of acetone photocatalytic oxidation, and they can account for the band at 2850 $cm^{-1}$ which is

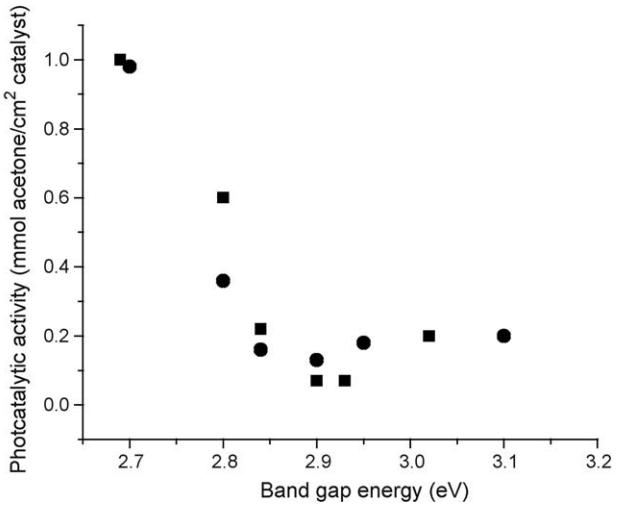


**Fig. 7.** Correlation between the photocatalytic activity of V/$TiO_2$(A) (●) and V/$TiO_2$(AR) (■) samples and band gap energy of the photocatalysts.

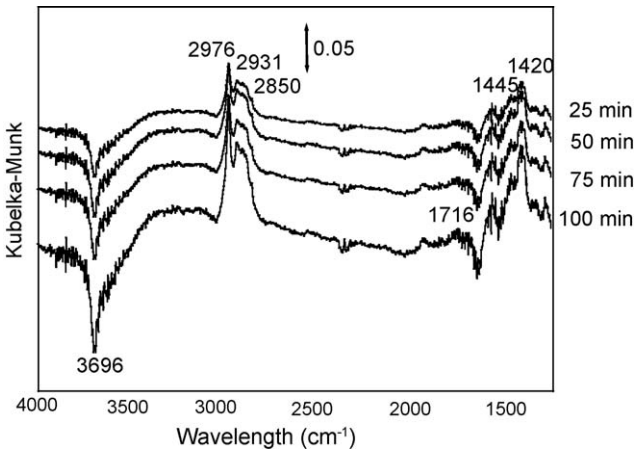


**Fig. 8.** DRIFT spectra of $V/TiO_2$ photocatalysts collected on different reaction time.

characteristic of the $\nu$(CH) vibration of aldehyde molecules. However, the reported frequency for acetaldehyde on $TiO_2$ [22,23], 1714 $cm^{-1}$, is closer to the value obtained in this study. The possible formation of acetic acid cannot be ascertained, because the corresponding $\nu$(CO) band overlaps with that of the acetone [20]. Changes in the $\nu$(OH) range of the spectra provide information concerning the role of adsorbed water in the photocatalytic oxidation of acetone. The band at 3696 $cm^{-1}$ decreases during reaction, this being a prove that the hydroxyl radicals, which are formed by trapping of a photogenerated hole by a hydroxyl group of the $TiO_2$, are the active species for the photocatalytic oxidation [3,24]. Consequently, the selective removal of the OH groups associated with the band at 3696 $cm^{-1}$ could represent their consumption following the hole trapping by acetone molecules.

## 4. Conclusions

The measurements have been carried out demonstrated that the deposition of vanadia using the dc-magnetron sputtering technique is providing active photocatalytic homogeneous spread thin films. Deposition of the vanadia films resulted homogeneously without any damage of the support surface. The resulted photocatalysts were active in decomposition of acetone under UV light radiation. Out of the UV range no acetone decomposition has been evidenced. The comparison of the two types of supports used in this study indicated the decomposition rate was smaller onto the pure anatase. A very good correlation between the band gap and the photocatalytic activity was determined indicating the positive effect of vanadia.

## Acknowledgments

The authors kindly acknowledge NATO's Scientific Affairs Division in the framework of the Science for Peace Programme Sfp 981476 for the financial support. One of the authors acknowledge the financial support from CNCSIS through the PN-II-RU-MC-2008-2 project (CNCSIS code 69) supervised by Ştefan Neaţu.

## References

[1] M.A. Fox, M.T. Dulay, Chem. Rev. 93 (1993) 341.
[2] A. Fujishima, T.N. Rao, D.A. Tryk, J. Photochem. Photobiol. C: Photochem. Rev. 1 (2000) 1.
[3] M.R. Hoffmann, S.T. Martin, W. Choi, D.W. Bahnemann, Chem. Rev. 95 (1995) 69.
[4] M. Anpo, M. Takeuchi, J. Catal. 216 (2003) 505.
[5] A.R. Bally, K. Prasad, R. Sanjinés, P.E. Schmid, F. Lévy, J. Benoit, C. Barthou, P. Benalloul, Mater. Res. Soc. Symp. 424 (1997) 471.
[6] A. Rotschild, F. Edelman, Y. Komem, F. Cosandey, Sens. Actuators B 67 (2000) 282.
[7] E. Comini, V. Guidi, C. Frigeri, I. Riccò, G. Sberveglieri, Sens. Actuators B 77 (2001) 16.
[8] P. Pichat, J. Disdier, C. Hoang-Van, D. Mas, G. Goutailler, C. Gaysse, Catal. Today 63 (2000) 363.
[9] J. Cunningham, G. Al-Sayyed, P. Sedlak, J. Caffrey, Catal. Today 53 (1999) 145.
[10] S. Malato, J. Blanco, C. Richter, M.I. Maldonado, Appl. Catal. B 25 (2000) 31.
[11] V.I. Pârvulescu, V. Marcu, in: R.M. Richards (Ed.), Surface and Nanomolecular Catalysis, CRC Press/Taylor and Francis Group, Boca Raton, FL, 2006 , p. 427 (Chapter 12).
[12] C. Minero, G. Marirlla, V. Maurino, E. Pelizzetti, Langmuir 16 (2000) 2632.
[13] C. Wang, D.F. Bahnemann, J.K. Dohrmann, Chem. Commun. (2000) 1539.
[14] A. Sclafani, M.N. Mozzanega, P. Pichat, J. Photochem. Photobiol. A: Chem. 59 (1991) 181.
[15] B. O'Regan, D.T. Schwartz, J. Appl. Phys. 80 (1996) 4749.
[16] J. Wang, S. Uma, K.J. Klabunde, Appl. Catal. B: Environ. 48 (2004) 151.
[17] W.N. Delgass, G.L. Haller, R. Kellerman, J.H. Lunsford, Spectroscopy in Heterogeneous Catalysis, Academic Press, New York, 1979.
[18] S.L. Murov (Ed.), Handbook of Photochemistry, Dekker, New York, 1973.
[19] W.C. Wu, C.C. Chuang, J.L. Lin, J. Phys. Chem. B 104 (2000) 8719.
[20] L.F. Liao, W.C. Wu, C.Y. Chen, J.L. Lin, J. Phys. Chem. B 105 (2001) 7678.
[21] N. Nagao, Y. Suda, Langmuir 5 (1989) 42.
[22] G.Y. Popova, T.V. Andrushkevich, Y.A. Chesalov, E.S. Stoyanov, Kinet. Catal. 41 (2000) 805.
[23] M.L. Sauer, D.F. Ollis, J. Catal. 158 (1996) 570.
[24] A. Linsebigler, G. Lu, J.T. Yates, Chem. Rev. 95 (1995) 735.
[25] G. Deo, I.E. Wachs, J. Catal. 129 (1991) 137.
[26] J.-M. Jehng, G. Deo, B.M. Weckhuysen, I.E. Wachs, J. Mol. Catal.: A Chem. 110 (1996) 41.
[27] M.A. Vuurman, I.E. Wachs, A.M. Hirt, J. Phys. Chem. 95 (1991) 9928.
[28] L. Kavan, M. Gratzel, S.E. Gilbert, C. Klemenz, H.J. Scheel, J. Am. Chem. Soc. 118 (1996) 6716.
[29] M. Yan, F. Chen, J. Zhang, M. Anpo, J. Phys. Chem. B 109 (2005) 8673.